Inorganic Chemistry

Article

pubs.acs.org/IC

Obtaining Chiral Metal–Organic Frameworks via a Prochirality Synthetic Strategy with Achiral Ligands Step-by-Step

Huan Dong, Hailiang Hu, Yang Liu, Jun Zhong, Guangju Zhang, Fangfang Zhao, Xuhui Sun, Youyong Li, and Zhenhui Kang*

Institute of Functional Nano & Soft Materials (FUNSOM), Jiangsu Key Laboratory for Carbon-based Functional Materials and Devices, and Collaborative Innovation Center of Suzhou Nano Science and Technology, Soochow University, Suzhou 215123, China

Supporting Information

ABSTRACT: Although some achievements of constructing chiral metal–organic frameworks (MOFs) with diverse achiral ligands have been made, there is still a lack of full understanding of the origin and formation mechanism of chirality, as well as the reasonable principles for the design and construction of chiral frameworks. The concept of prochirality in organic molecules and complex systems inspires us to explore the synthetic strategy of chiral MOFs based on achiral sources. Here, an achiral compound $[Cu(en)][(VO_3)_2]$ (**1**) was isolated in the $CuCl_2/NH_4VO_3$/en system, while further chiral frameworks $[Cu(en)(Im)_2][(VO_3)_2]$ (**2a** and **2b**) were obtained by the reaction between compound **1** and another achiral ligand Im (ethanediamine = en and imidazole = Im). In the present system, compound **1** has the characteristic of a quasi-plane structure unit. Further reaction of compound **1** and the achiral ligand (Im) induced the formation of chiral Λ/Δ Cu centers, and then a pair of chiral frameworks containing one-dimensional (1D) helical chains was formed. The chiral symmetry breaking phenomenon of compounds **2a** and **2b** can also be expected and explained based on this kind of prochirality synthetic strategy.

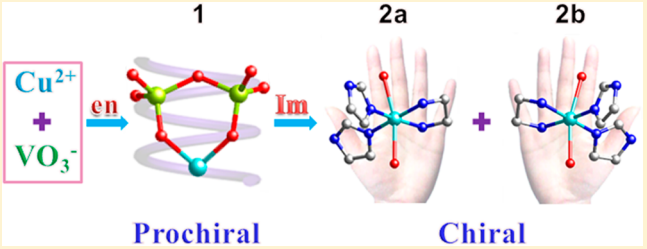

INTRODUCTION

Chiral metal–organic frameworks (MOFs) have been attracting attention not only because of their intriguing variety of architectures and topologies[1−3] but also owing to their potential applications in the aspects of enantioselective catalysis,[4−6] chiral separation,[7−9] nonlinear optics,[10−12] and magnetism.[13−15] The design and construction of chiral MOFs can be achieved through two main approaches. One is based on the use of chiral sources (chiral organic linkers or metal complexes),[16−18] while the other is developing achiral precursors into chiral materials under spontaneous resolution.[19−23] Building chiral MOFs with enantiopure ligands appears to be a straightforward strategy, but it always suffers from complex synthesis and structure limitations of enantiopure ligands. Also, although some achievements of constructing chiral MOFs with diverse achiral ligands have been made,[24−31] there is still a lack of full understanding of the origin and formation mechanism of chirality, as well as the reasonable principles for the design and construction of chiral frameworks.[32]

For understanding of the chiral structure, the concept of prochirality was introduced by Hanson in 1966.[33] It was widely used for organic molecules and then extended to mononuclear octahedral, square pyramidal, square planar, and trigonal bipyramidal coordination compounds.[34−40] Typically, a prochiral coordination compound is characterized by a prochiral center and/or by the existence of two heterotopic elements that can be ligands, faces, or planes, depending on the geometry of the complex. For each of these elements, a reaction can be identified that transforms the prochiral metal center into a chiral center. In particular, an enantiomeric product having opposite chirality at the metal atom can be formed by replacement of either one of the enantiotopic ligands by a different achiral ligand, addition of the same achiral ligand to either one of the two enantiotopic faces, or ligand rearrangement along either one of the two enantiotopic planes.[41−44] The concept of prochirality for coordination compounds improves the development of asymmetric synthesis and bioinorganic chemistry significantly,[45−48] which inspires us to explore the synthetic strategy of chiral MOFs based on achiral sources.

Here, we demonstrate construction of chiral frameworks via a prochirality synthetic strategy with simple and common achiral ligands ethanediamine (en) and imidazole (Im) step-by-step. First, an achiral compound $[Cu(en)][(VO_3)_2]$ (**1**) was synthesized with an achiral ligand en, which has the characteristics of a quasi-helical structure containing a quasi-plane structure unit and a proposed prochiral center. The further surface reaction between **1** and the second achiral ligand Im induced the formation of chiral Λ/Δ Cu centers, and then a pair of chiral frameworks $[Cu(en)(Im)_2][(VO_3)_2]$ (**2a** and **2b**) containing one-dimensional (1D) helical chains was formed. Moreover, the chiral symmetry breaking phenomenon of compounds **2a** and **2b** can also be expected and explained

Received: November 18, 2013
Published: March 10, 2014

   dx.doi.org/10.1021/ic402867x | Inorg. Chem. 2014, 53, 3434−3440

based on this kind of prochirality synthetic strategy and the structural characteristic of the prochiral center in compound **1**.

EXPERIMENTAL SECTION

Materials and Methods. All materials were reagent grade obtained from commercial sources and used without further purification. Elemental analyses (C, H, and N) were performed using an EA1110 elemental analyzer. The IR spectra were recorded in the range of 400−4000 cm^{-1} on a Fourier transform IR spectrometer as KBr pellets. The thermogravimetric analyses (TGA) were carried out using a Universal Analysis 2000 thermogravimetric analyzer (TGA) in N_2 with a heating rate of 10 °C/min. Powder X-ray diffraction (PXRD) data were collected on an X'Pert-ProMPD (Holand) D/max-γA X-ray diffractometer with Cu Kα radiation in a flat plate geometry. X-ray absorption near edge structure (XANES) and extended X-ray absorption fine structure (EXAFS) data were collected on beamline 14W at the Shanghai Synchrotron Radiation Facility. Electrochemical test experiments were performed with an IM6e potentiostat (Zahner Elektrik Company, Germany) in a conventional three-electrode cell. A saturated calomel electrode (SCE) was used as a reference electrode, and a Pt wire was used as a counter electrode. Chemically bulk-modified carbon paste electrodes (CPEs) were used as the working electrodes. The Raman spectra were collected on an HR 800 Raman spectroscope (J Y, France) equipped with a synapse CCD detector and a confocal Olympus microscope. The spectrograph uses 600 g mm^{-1} gratings and a 633 nm He−Ne laser. The circular dichroism (CD) spectra were recorded on a JASCOJ-810 spectropolarimeter with KBr pellets.

Synthesis of [Cu(en)][$(VO_3)_2$] (1). In our experiments, compound **1** was prepared by the hydrothermal method. A mixture of NH_4VO_3 (0.06 g, 0.5 mmol), $CuCl_2·2H_2O$ (0.085 g, 0.5 mmol), and en (0.1 mL, 1.49 mmol) was dissolved in 12.0 mL of distilled water and stirred briefly for 0.5 h. When the pH value was adjusted to approximately 5.5 by dilute HCl solution, the mixture was transferred to and sealed in a 22 mL Teflon-lined stainless steel container, which was heated at 150 °C for 72 h. After being cooled to room temperature unaffectedly, green block crystals of **1** were filtered and washed with distilled water (yield about 30% based on Cu). Elemental analyses calculated for **1**: C, 7.47; H, 2.51; N, 8.71. Found: C, 7.52; H, 2.49; N, 8.68. IR (KBr pellet, cm^{-1}): 3315 (m), 1574 (m), 1043 (s), 945 (s), 865(s), 777 (s), 640 (s).

Synthesis of [Cu(en)$(Im)_2$][$(VO_3)_2$] (2). A mixture of compound **1** (0.16 g, 0.5 mmol), Im (0.1 g, 1.5 mmol), and H_2O (12 mL) was adjusted to approximately pH 7.5 with dilute en solution and HCl and stirred for 0.5 h and then transferred to and sealed in a 22 mL Teflon-lined stainless steel container, which was heated at 150 °C for 72 h and then cooled to room temperature naturally. Blue rodlike crystals of **2** existed on the surface of **1**, and they were peeled off compound **1** and washed with distilled water. The mixture **2** was comprised of both **2a** and **2b**, which could be separated manually under a polarized light microscope (yield about 18% based on Cu). Elemental analyses calculated for **2**: C, 20.99; H, 3.53; N, 18.37. Found: C, 21.06; H, 3.49; N, 18.42. IR (KBr pellet, cm^{-1}): 3103 (m), 1574 (m), 1324 (s), 937 (s), 827(w), 780 (s), 653 (s).

X-ray Crystallographic Study. Crystal data for compounds **1**, **2a**, and **2b** were collected on a Bruker APEX-II CCD diffractometer with Mo Kα radiation (λ = 0.71073 Å). The structures were solved by the direct methods and refined by full-matrix least-squares on F^2 using the *SHELXTL* crystallographic software package.[49,50] All non-hydrogen atoms were refined anisotropically, and hydrogen atoms of the en and Im molecules were generated theoretically onto the specific atoms and refined isotropically with fixed thermal factors. A summary of the crystallographic data and structure refinement details for these three compounds are given in Table 1, selected bond distances and angles are given in Table S1, Supporting Information, and 10 typical crystal data and structure refinements of **2** are given in Table 2. CCDC numbers are 905137−905139 for **1**−**2b**, respectively.

Preparation of 1-CPE. Electrochemical measurements were carried out in a conventional three-electrode electrochemical cell. A total of 0.1 g of graphite powder and 10 mg of compound **1** were mixed and ground together by agate mortar and pestle to achieve an even and dry mixture. To the mixture, 0.3 mL of nujol was added and stirred with a glass rod. Then the homogenized mixture was used to pack the glass tubes with 5 mm inner diameter, and the surface was wiped with weighing paper. Electrical contact was established with copper rod through the back of the electrode. In a similar manner, bare CPE was made only with graphite powder.

Table 1. Crystal Data and Structure Refinements for Compounds 1, 2a, and 2b

compound	1	2a	2b
empirical formula	$C_2H_8CuN_2O_6V_2$	$C_8H_{16}CuN_6O_6V_2$	$C_8H_{16}CuN_6O_6V_2$
formula weight	321.52	457.69	457.69
crystal system	monoclinic	orthorhombic	orthorhombic
space group	$P2_1/n$	$P2_12_12_1$	$P2_12_12_1$
a (Å)	5.7771(2)	10.6943(17)	10.6820(7)
b (Å)	8.1522(3)	11.6521(19)	11.6044(7)
c (Å)	17.5012(7)	12.834(2)	12.6888(8)
α (deg)	90.00	90.00	90.00
β (deg)	90.451(1)	90.00	90.00
γ (deg)	90.00	90.00	90.00
V (Å^3)	824.21(5)	1599.3(4)	1572.88(17)
Z	4	4	4
D_c (g cm^{-3})	2.591	1.901	1.933
μ (mm^{-1})	4.777	2.500	2.542
F(000)	628.0	916.0	916.0
collcd reflns	7291	8483	13426
unique reflns	2025	3983	3866
parameters	118	208	208
R_{int}	0.0177	0.0218	0.0202
GOF	1.116	0.967	1.011
$R_1{}^a$ [$I > 2\sigma(I)$]	0.0189	0.0241	0.0161
$wR_2{}^b$ (all data)	0.0506	0.0501	0.0399
Flack parameter		0.000(11)	0.018(8)

$^aR_1 = \Sigma||F_0| - |F_c||/\Sigma|F_0|$. $^bwR_2 = \Sigma[w(F_0^2 - F_c^2)^2]/\Sigma[w(F_0^2)^2]^{1/2}$.

RESULTS AND DISCUSSION

Single-crystal analysis reveals that **1** is centrosymmetric and belongs to the monoclinic system with space group $P2_1/n$. The unit cell is composed of one Cu^{2+} ion, one $[V_2O_6]^{2-}$ anion, and one en molecule, as shown in Figure 1a. There are two crystal independent V centers of V1 and V2 in the structure. Each V center is surrounded by four O atoms in tetrahedral geometry. Here, two VO_4 tetrahedrons of the V1 and V2 centers link together to generate a $[V_2O_6]^{2-}$ anion. Furthermore, such $[V_2O_6]^{2-}$ anions link to each other end-to-end in corner-sharing mode, forming an infinite 1D chain with a quasi-helical structure along the a axis (Figure S1, Supporting Information). The Cu center adopts a distorted octahedral geometry of CuN_2O_4 unit, which is completed by two N atoms from one en molecule and four O atoms from three $[V_2O_6]^{2-}$ anions (Figure S2, Supporting Information). Two symmetrically equivalent CuN_2O_4 units are bridged together by terminal oxygen atoms (O1) from vanadium oxygen chains, generating a binuclear secondary building unit (SBU). Each CuN_2O_4 unit is connected to three vanadium oxygen chains, while each binuclear SBU is in connection with four (Figure 1b). This kind of connection develops the whole net into a 2D bilayer

dx.doi.org/10.1021/ic402867x | Inorg. Chem. 2014, 53, 3434−3440

Table 2. Ten Crystal Data and Structure Refinements for Compound 2

	a (Å)	*b* (Å)	*c* (Å)	*V* (Å^3)	Flack	chirality
1	10.6943(17)	11.6521(19)	12.834(2)	1599.3(4)	0.000(11)	L
2	10.6820(7)	11.6044(7)	12.6888(8)	1572.88(17)	0.018(8)	D
3	10.6889(14)	11.6126(15)	12.6969(17)	1576.0(4)	−0.01(2)	D
4	10.6916(15)	11.6172(18)	12.6878(19)	1575.9(4)	0.006(17)	D
5	10.683(3)	11.598(4)	12.703(4)	1573.9(9)	0.010(12)	D
6	10.6967(12)	11.6229(13)	12.7097(14)	1580.2(3)	−0.002(15)	L
7	10.6937(10)	11.6164(11)	12.6973(11)	1577.3(3)	0.005(14)	L
8	10.6846(15)	11.6016(17)	12.6915(18)	1573.2(4)	0.028(15)	L
9	10.649(5)	11.556(5)	12.642(6)	1555.7(12)	0.033(17)	L
10	10.669(3)	11.575(3)	12.673(3)	1565.0(7)	0.009(19)	L

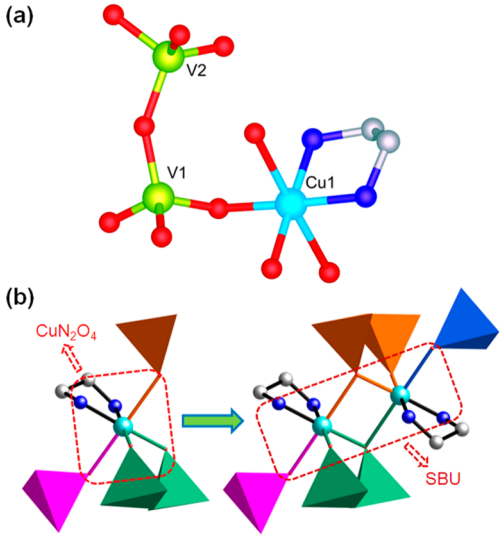

Figure 1. (a) The asymmetric unit of **1** with partial atoms labeling scheme. (b) The CuN_2O_4 unit and binuclear SBU connect to vanadium oxygen chains (different color polyhedrons represent different chains).

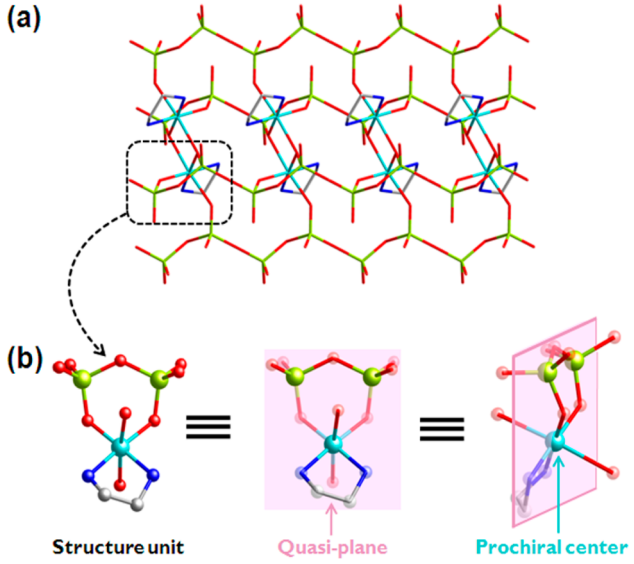

Figure 2. (a) The 2D bilayer structure of **1**. (b) The structure unit containing a quasi-plane and a prochiral center.

structure (Figure S3, Supporting Information), and then these parallel bilayers are arranged alternately in a ABAB pattern through hydrogen-bonding interactions, generating a 3D supramolecular network (Figure S4, Supporting Information).

A closed observation shows that another kind of structure unit exists in the present 2D bilayer (Figure 2a), which is a $CuN_2C_2O_9V_2$ unit (Figure 2b left). Here, if a proposed plane is made up running through the Cu and V atoms in this unit, most of the atoms which surround the Cu atom are close to this plane, and then this plane (the pink plane in Figure 2b middle) can be regarded as the quasi-plane in the present unit. It is precisely the central location of Cu atom in the unit; thus, if a reaction occurred between Cu and a new ligand with stronger coordination ability, the symmetry of CuN_2O_4 unit would be destroyed, and a chiral center might be formed. Therefore, the Cu atom could be regarded as a prochiral center (Figure 2b right), which is expected to provide a possibility for the achievement of chirality in the whole framework.

General speaking, ligand Im has strong coordination ability to form a coordination bond (Cu−N) with the Cu ion. Thus, in the following experimental design, the second achiral ligand Im was introduced, and the mixture of Im, compound **1**, and H_2O was treated in a hydrothermal condition. As expected, compounds **2** were prepared on the basis of **1**: blue rodlike crystals of compounds **2** were obtained on the surface of compound **1** (Figure S5). Structure analyses reveal that **2a** and **2b** are enantiomers, which crystallize in the same chiral space group $P2_12_12_1$. The Flack parameters of **2a** and **2b** are 0.000(11) and 0.018(8), respectively. Here, a detailed description of **2a** will be exhibited as an example. The asymmetric unit of **2a** consists of one Cu^{2+} ion, one $[V_2O_6]^{2-}$ anion, one en molecule, and two Im ligands (Figure 3). Each Cu center displays a slightly distorted octahedral geometry with chiral Λ configuration, which is coordinated by four N atoms from two Im and one en molecules, and two O atoms from two $[V_2O_6]^{2-}$ anions. On the contrary, the Cu center adopts the Δ absolute configuration in **2b** (Figure 4a). The unique V1 and V2 centers, which are similar to those in **1**,

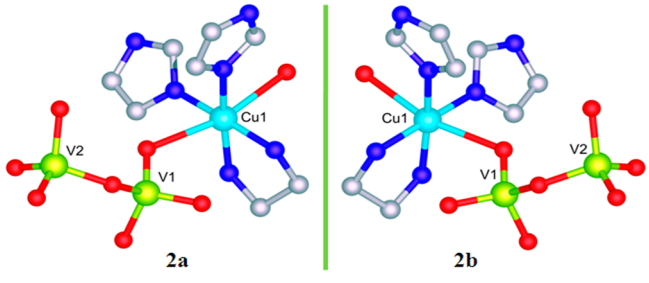

Figure 3. The asymmetric units of **2a** and **2b** with partial atoms labeling scheme.

dx.doi.org/10.1021/ic402867x | *Inorg. Chem.* 2014, 53, 3434−3440

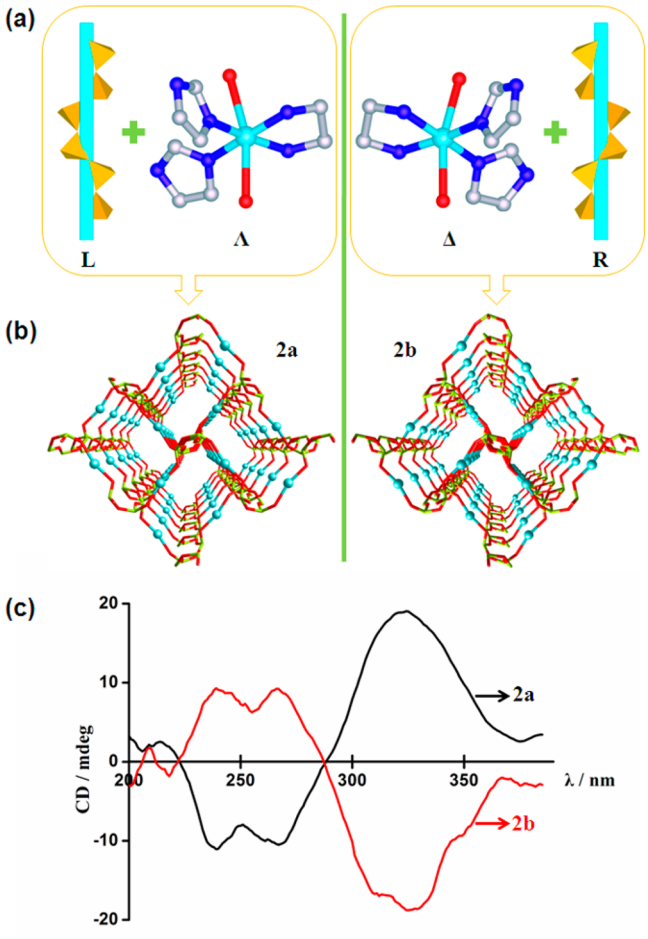

Figure 4. (a) The helices and absolute configuration of chiral metal center in **2a** (left) and **2b** (right). (b) The 3D chiral frameworks of **2a** and **2b**. All ligands and H atoms are omitted for clarity. (c) Solid state CD spectra of **2a** (black) and **2b** (red) in KBr pellets.

adopt tetrahedral geometries with four O atoms, and these tetrahedrons are linked each other to generate a chainlike structure. Note that due to the screw coordination arrangement of the achiral en and Im ligands around the Cu^{2+} ion, the chiral $[Cu(en)(Im)_2]^{2+}$ complex with a Λ configuration allows the control of the absolute helicity of the V−O chain. Herein, after passing through an intermediate quasi-helical state in **1**, such vanadium oxygen chains turn into a real helical structure in **2**, and left- and right-hand helices only appeared in **2a** and **2b**, respectively. These helical chains are linked by chiral centers to yield three-dimensional (3D) networks (Figure 4b), and then the chirality is transferred from the center to the whole crystal, forming a pair of chiral frameworks. To validate the chiral properties of **2a** and **2b**, CD spectra were recorded. Compounds **2** are insoluble in water and common organic solvents; the CD spectra were investigated from KBr pellets. As shown in Figure 4c, the CD spectra of compounds **2a** and **2b** are almost mirror images of each other, indicating that the pair of compounds are enantiomers.[51] In the wavelength range from 200 to 350 nm, **2a** shows positive Cotton effects at λ = 239 and 267 nm and a negative Cotton effect at 324 nm. Compound **2b** shows Cotton effects of the opposite signs to **2a** at nearly identical wavelengths (239, 266, and 325 nm respectively).

Then, compounds **1** and **2** were characterized by PXRD patterns, IR spectra, and TG analyses (Figures S6−S9, Supporting Information). Here, the question is whether the production of chiral compounds is a reaction based on a prochiral center or a process of dissolution−recrystallization. The former can indicate that a prochiral strategy could be used to design and synthesize a chiral structure of a coordination polymer, while the other is only a common self-assembly process of a black box.

The reaction process between **1** and Im aqueous solution was monitored and recorded under ambient conditions. As shown in Figure 5a, with increasing the reaction time from 0 to 4 h, a kind of blue crystal gradually grew on the surface of **1**. When the reaction proceeded for 6 h, a mass of blue crystal

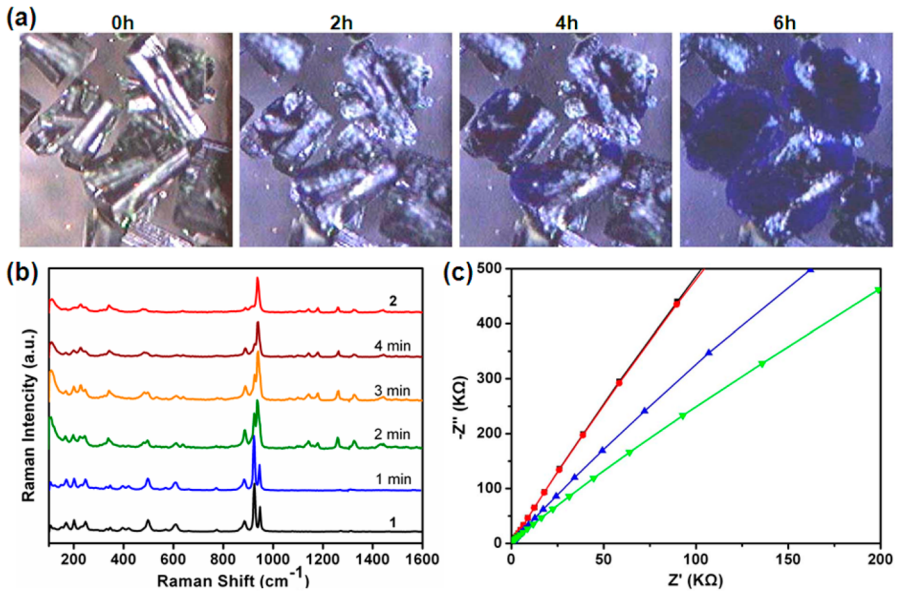

Figure 5. (a) In-situ observation of compound **1** reacted with Im solution under ambient conditions at different time periods, showing the generating process of blue crystal. (b) In-situ Raman spectra from bottom to top: pure **1** (black), **1** and Im solution (blue, green, orange and rufous) and pure **2** (red) under air. (c) EIS of 1-CPE (green and blue curve for 1-CPE with and without Im, respectively) and bare CPE (black and red curve for with and without Im, respectively) in 0.5 M Na_2SO_4 solution.

dx.doi.org/10.1021/ic402867x | Inorg. Chem. 2014, 53, 3434−3440

appeared and aggregated together. PXRD indicated that the pattern of blue crystal corresponds well with the simulated result from the single crystal data of **2** (Figure S10, Supporting Information). The above-mentioned reaction process was also monitored by in situ Raman spectra. In Figure 5b, black and red curves represent the Raman signal of pure compounds **1** and **2**, respectively. The emergence of a series of characteristic peaks in the range of 1100−1500 cm^{-1} was owed to Im. While the bands at 920−950 cm^{-1} should correspond to V−O vibrations, and the peaks at lower wavenumbers (below 800 cm^{-1}) mainly belong to the oscillations of the V−O−V framework.[52,53] When a little bit of Im solution was added to the powder of **1**, significant changes in the Raman spectra were observed within 3 min, and the spectrum recorded after 4 min is highly similar to that of pure **2**. In our further experiments, the reaction between **1** and Im was analyzed by electrochemical impedance spectroscopy (EIS), a method of characterizing the electrode surface by measuring the impedance changes. Figure 5c shows the Nyquist plots of the different processes of **1** modified carbon paste electrode (1-CPE) and bare CPE in Na_2SO_4 electrolyte. The arc radius on the EIS Nyquist plot of 1-CPE in Na_2SO_4 mixed with Im (0.5 mL, 0.08 M) (green curve) is smaller than that of 1-CPE (blue curve) without Im, indicating a fast interfacial charge transfer between **1** and Im. While the EIS curves of the bare CPE in Na_2SO_4 with (black curve) and without Im (red curve) are almost entirely overlapped, meaning the little influence of Im on bare CPE.

Although the above Raman and electrochemical results showed that **1** can react quickly with Im and compounds **2** (**2a** and **2b**) can be formed on its surface, there is still a question here of whether the formation of **2** is based on a dissolution−reaction process (self-assembly from the basic anions and ligands) or a purely surface reaction process. To further prove the above reaction process is not the simple self-assembly process, a series of control experiments were carried out. We further compared the blue solution obtained from the reaction of Im and **1** (aq-1, Figure 6a inset) and another blue solution formed from raw materials (a mixture of NH_4VO_3, $CuCl_2 \cdot 2H_2O$, en and Im was dissolved in distilled water, and the molar ratio of these reactants was consistent with the proportion of each component in the structure of compound **2**; aq-2, Figure 6a inset) by Raman spectrum technique. In Figure 6a, the Raman spectrum of aq-1 (aqua line) has the typical characteristic peaks of compound **2** (red line), while that for aq-2 (azure line) was totally different from either **1** (black) or **2** (red). Further, two powder samples (powder-1 and -2, Figure 6b inset) were obtained by drying those above two blue solutions (aq-1 and -2) at ambient temperature respectively. The PXRD patterns in Figure 6b further proved that the peak positions of the powder-1 (aqua) derived from aq-1 correspond well with that of compound **2** (red), while powder-2 (azure) had no connection with **1** (black) and **2** (red). The above results demonstrated that aq-1 contains the only component of **2** and is totally different from the mixture of reactants.

X-ray absorption spectroscopy (XAS) is an element-specific spectroscopic technique involving the excitation of electrons from a core level to the empty states and is particularly powerful to get structural information of different species. In the followed experiments, XAS experiments (X-ray absorption near edge structure, XANES; extended X-ray absorption fine structure, EXAFS) were performed to investigate the electronic structure of Cu in **1** (both in solid state and in situ reaction with Im solution). Cu K-edge XANES and EXAFS data for **1**

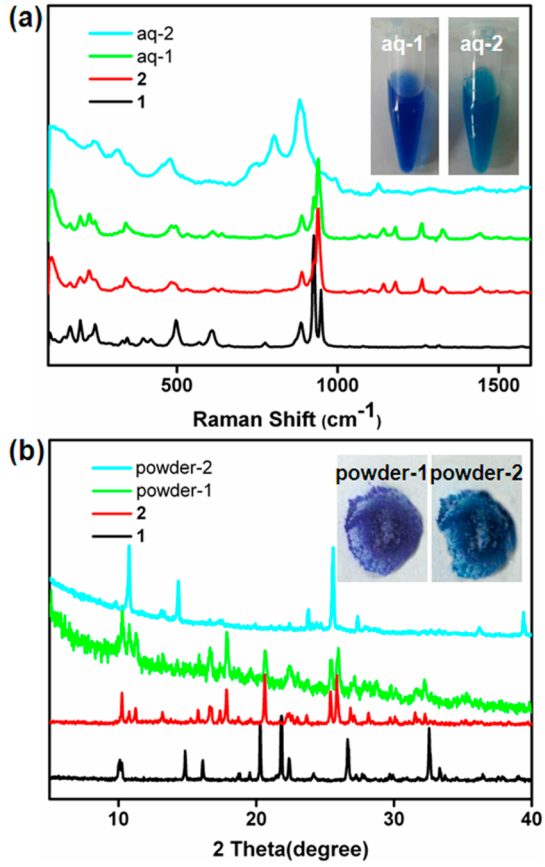

Figure 6. (a) Raman spectra and (b) PXRD patterns from bottom to top: compound **1** (black), compound **2** (red), aq-1 and powder-1 (aqua) obtained from the reaction of Im and **1**, and aq-2 and powder-2 (azure) mixed by reactants. The insets show the aq and powder samples.

(both in solid and the in situ reaction between **1** and Im solution) have been collected and are shown in Figure 7. The XANES data for **1** in solid and in situ reaction conditions have a very similar spectral shape. The EXAFS data in R space (the inset in Figure 7) for Cu before adding solution shows a strong peak for Cu−N/Cu−O bonds. Since Cu−N bonds and Cu−O

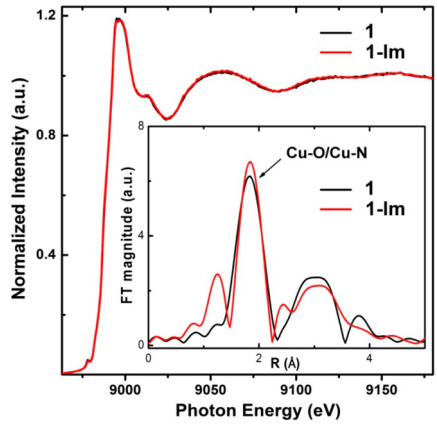

Figure 7. Cu K-edge XANES spectra of **1**, the black and red curve for pure **1** and under the in situ reaction (with Im) condition, respectively. The inset shows the corresponding Fourier transform of the EXAFS data.

dx.doi.org/10.1021/ic402867x | Inorg. Chem. 2014, 53, 3434−3440

bonds show almost the same bond length in R space, there is only one main peak in the spectra consistent with the crystal structure. When the Im solution was added, the EXAFS data for Cu show almost identical Cu−N/Cu−O bonds with **1** (in solid) in R space. Here, we measured the XAS spectra just after the Im solution was added, and the spectra can be repeated several minutes later. During the reaction process, if **1** could solve in the solution and form the basic anions and ligands, the composites should show a new solution state and the XANES spectrum could be different from that for **1**. All of the above Raman and PXRD results as well as the XANES spectra and EXAFS data suggest that the formation of **2** should via a reaction directly occur on the solid surface and without a self-assembly process from the basic anions and ligands.

In the present system, **2a** and **2b** show the same color and shape in nature light but exhibit light purple and dark blue in the presence of polarized light, respectively (typical photo images of **2a** and **2b** shown in Figure 8a). Therefore, the pairs

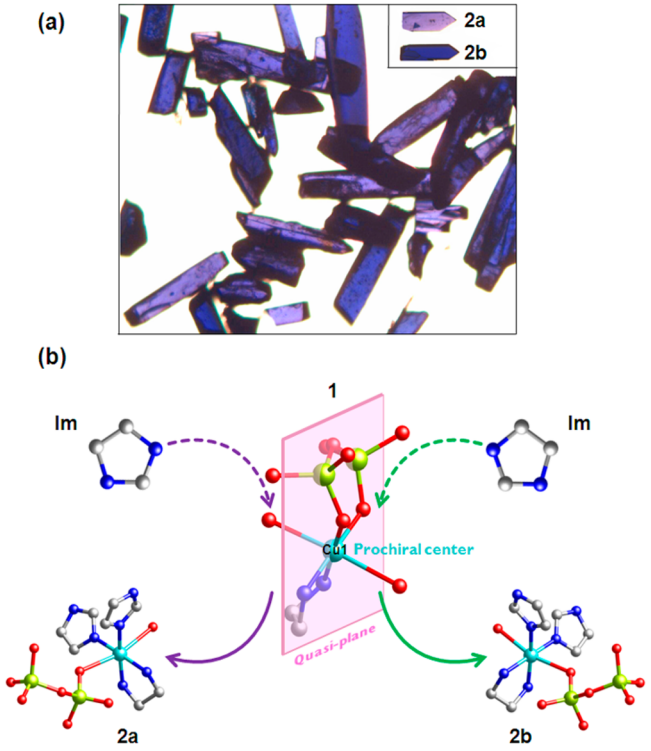

Figure 8. (a) Photographs of compounds **2a** (light purple) and **2b** (dark blue) viewed in the presence of polarized light by using a polarized light microscope, among them, a little more **2a** than **2b**. (b) Possible mechanisms of the chiral symmetry breaking phenomenon. Light pink plane is the proposed quasi-plane through the Cu atom in the structure unit, which is both the reaction hotspot and the prochiral center in **1**.

of enantiomers can be separated manually. In following experiments, it was found that the probabilities of **2a** and **2b** had a distinction that was close to 6:4 (10 typical crystal data and structure refinements of **2** are shown in Table 2). It inspired us carried out a further detailed structural analysis of the proposed prochiral center in **1**. As shown in Figure 8b, the Cu atom being on the quasi-plane has a relatively symmetrical coordination environment, which makes the Cu atom an expected hotspot here. The left space is exactly exposed and there is a binuclear SBU on the right side of the quasi-plane in the framework of **1** (Figure 9). So it can be supposed, when the second ligand Im was introduced, the attack/substitution

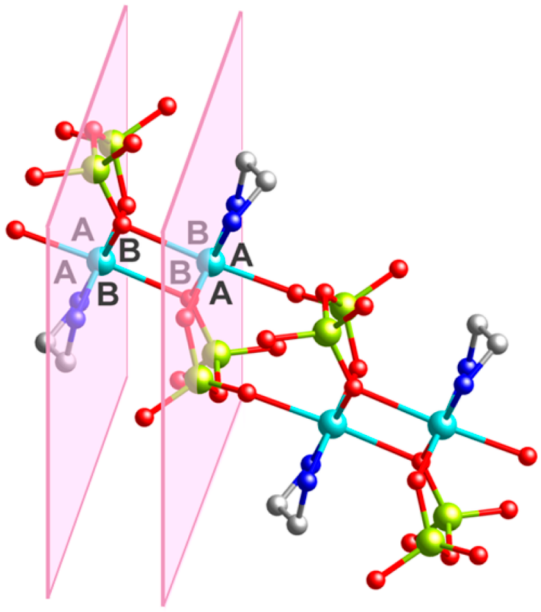

Figure 9. Both sides of quasi-plane are marked with **A** and **B** respectively. Site **A** is significantly larger than site **B**.

reaction process occuring in the hotspot on the left is inevitably much easier than the right. On the basis of the experimental results (**2a** and **2b**), we speculated that Im attack the Cu hotspot on the left side of the quasi-plane could produce **2a**, and oppositely **2b** could be obtained. Our interpretation and theory are still very rough currently; nevertheless, they offer a simple and back-up model to understand the architectures of MOFs and other frameworks, along with the design and forming process of chirality. Considering the diversity of MOFs and other frameworks, as well as the complexity and uncertainty of the self-assembly process, the possible structural characteristic and hotspots (maybe definite chemical bond/cluster/chain, large anion or cation, etc.) still need to be further clarified.

CONCLUSION

In summary, we demonstrated the construction of chiral frameworks via prochirality synthetic strategy with achiral ligands step by step. Compound **1** with a quasi-helical structure is the prior product to chiral enantiomers **2a** and **2b**, which can be synthesized via further surface reaction between compound **1** and Im. The chiral symmetry breaking phenomenon of compounds **2a** and **2b** can also be explained based on this kind of prochirality synthetic strategy and the prochiral structural characteristic of compound **1**. More achiral ligands (such as 1,3-propane diamine, 1,2,4-triazole, etc.) with different coordination abilities and more metal ions (such as Co^{2+}, Ag^{+}, Zn^{2+}, Ni^{2+}, etc.) could be helpful for the design and fabrication of various functional chiral crystalline materials.

ASSOCIATED CONTENT

Supporting Information

X-ray crystallographic information files (CIF); table of selected bond lengths and angles; and additional figures of compounds

dx.doi.org/10.1021/ic402867x | Inorg. Chem. 2014, 53, 3434−3440

1 and 2; together with PXRD, IR and TGA. This material is available free of charge via the Internet at http://pubs.acs.org.

AUTHOR INFORMATION

Corresponding Author

*E-mail: zhkang@suda.edu.cn.

Notes

The authors declare no competing financial interest.

ACKNOWLEDGMENTS

This work is supported by the National Basic Research Program of China (973 Program) (2012CB825800, 2013CB932702), the National Natural Science Foundation of China (No. 51132006), the Specialized Research Fund for the Doctoral Program of Higher Education (20123201110018), a Suzhou Planning Project of Science and Technology (ZXG2012028), and a project funded by the Priority Academic Program Development of Jiangsu Higher Education Institutions.

REFERENCES

(1) Lukin, O.; Kubota, T.; Okamoto, Y.; Kaufmann, A.; Vogtle, F. *Chem.—Eur. J.* **2004**, *10*, 2804.
(2) (a) Morris, R. E.; Bu, X. H. *Nat. Chem.* **2010**, *2*, 353. (b) Goldberg, I. *CrystEngComm.* **2008**, *10*, 637.
(3) Zhang, Y.; He, X. W.; Zhang, J.; Feng, P. Y. *Cryst. Growth Des.* **2011**, *11*, 29.
(4) Seo, J. S.; Whang, D.; Lee, H.; Jun, S. I.; Oh, J.; Jeon, Y. J.; Kim, K. *Nature* **2000**, *404*, 982.
(5) Nomiya, K.; Takahashi, S.; Noguchi, R.; Nemoto, S.; Takayama, T.; Oda, M. *Inorg. Chem.* **2000**, *39*, 3301.
(6) Ma, L.; Abney, C.; Lin, W. *Chem Soc. Rev.* **2009**, *38*, 1248.
(7) Kim, K.; Banerjee, M.; Yoon, M.; Das, S. In *Functional Metal-Organic Frameworks: Gas Storage, Separation and Catalysis*; Schroder, M., Ed.; Springer-Verlag: Berlin, 2010; Vol. *293*, p 115.
(8) Li, G.; Yu, W.; Cui, Y. *J. Am. Chem. Soc.* **2008**, *130*, 4582.
(9) Das, M. C.; Guo, Q. S.; He, Y. B.; Kim, J.; Zhao, C. G.; Hong, K. L.; Xiang, S. C.; Zhang, Z. J.; Thomas, K. M.; Krishna, R.; Chen, B. L. *J. Am. Chem. Soc.* **2012**, *134*, 8703.
(10) Duan, X.; Meng, Q.; Su, Y.; Li, Y.; Duan, C.; Ren, X.; Lu, C. *Chem.—Eur. J.* **2011**, *17*, 9936.
(11) Evans, O. R.; Lin, W. B. *Acc. Chem. Res.* **2002**, *35*, 511.
(12) Wang, C.; Zhang, T.; Lin, W. *Chem. Rev.* **2012**, *112*, 1084.
(13) Taguchi, Y.; Oohara, Y.; Yoshizawa, H.; Nagaosa, N.; Tokura, Y. *Science* **2001**, *291*, 2573.
(14) Train, C.; Gruselle, M.; Verdaguer, M. *Chem. Soc. Rev.* **2011**, *40*, 3297.
(15) Train, C.; Gheorghe, R.; Krstic, V.; Chamoreau, L. M.; Ovanesyan, N. S.; Rikken, G. L. J. A.; Gruselle, M.; Verdaguer, M. *Nat. Mater.* **2008**, *7*, 729.
(16) (a) Meggers, E. *Eur. J. Inorg. Chem.* **2011**, 2911. (b) Gautier, R.; Norquist, A. J.; Poeppelmeier, K. R. *Cryst. Growth Des.* **2012**, *12*, 6267.
(17) Kamikawa, K. *J. Synth. Org. Chem. Jpn.* **2008**, *66*, 953.
(18) Arae, S.; Ogasawara, M. *J. Synth. Org. Chem. Jpn.* **2012**, *70*, 593.
(19) Chen, W. L.; Tan, H. Q.; Wang, E. B. *J. Coord. Chem.* **2012**, *65*, 1.
(20) Pérez-García, L.; Amabilino, D. B. *Chem. Soc. Rev.* **2007**, *36*, 941.
(21) (a) Zhang, J.; Chen, S. M.; Wu, T.; Feng, P. Y.; Bu, X. H. *J. Am. Chem. Soc.* **2008**, *130*, 12882. (b) Zhang, J.; Chen, S. M.; Nieto, R. A.; Wu, T.; Feng, P. Y.; Bu, X. H. *Angew. Chem., Int. Ed.* **2010**, *49*, 1267. (c) Wang, F.; Shu, Y. B.; Bu, X. H.; Zhang, J. *Chem.—Eur. J.* **2012**, *18*, 11876.
(22) Weissbuch, I.; Lahav, M. *Chem. Rev.* **2011**, *111*, 3236.
(23) Hasenknopf, B.; Micoine, K.; Lacôte, E.; Thorimbert, S.; Malacria, M.; Thouvenot, R. *Eur. J. Inorg. Chem.* **2008**, *2008*, 5001.
(24) Lan, Y. Q.; Li, S. L.; Su, Z. M.; Shao, K. Z.; Ma, J. F.; Wang, X. L.; Wang, E. B. *Chem. Commun.* **2008**, 58.
(25) Lan, Y. Q.; Li, S. L.; Wang, X. L.; Shao, K. Z.; Du, D. Y.; Su, Z. M.; Wang, E. B. *Chem.—Eur. J.* **2008**, *14*, 9999.
(26) (a) Li, J. R.; Yu, Q.; Tao, Y.; Bu, X. H.; Ribas, J.; Batten, S. R. *Chem. Commun.* **2007**, 2290. (b) Li, J. R.; Tao, Y.; Yu, Q.; Bu, X. H.; Sakamoto, H.; Kitagawa, S. *Chem.—Eur. J.* **2008**, *14*, 2771.
(27) Yan, B. B.; Capracotta, M. D.; Maggard, P. A. *Inorg. Chem.* **2005**, *44*, 6509.
(28) Tong, X. L.; Hu, T. L.; Zhao, J. P.; Wang, Y. K.; Zhang, H.; Bu, X. H. *Chem. Commun.* **2010**, *46*, 8543.
(29) Li, Y. W.; Tao, Y.; Wang, L. F.; Hu, T. L.; Bu, X. H. *RSC Adv.* **2012**, *2*, 4348.
(30) Gao, E. Q.; Yue, Y. F.; Bai, S. Q.; He, Z.; Yan, C. H. *J. Am. Chem. Soc.* **2004**, *126*, 1419.
(31) Zheng, X. D.; Zhang, M.; Jiang, L.; Lu, T. B. *Dalton Trans.* **2012**, *41*, 1786.
(32) (a) Maggard, P. A.; Stern, C. L.; Poeppelmeier, K. R. *J. Am. Chem. Soc.* **2001**, *123*, 7742. (b) Maggard, P. A.; Kopf, A. L.; Stern, C. L.; Poeppelmeier, K. R. *CrystEngComm.* **2004**, *6*, 452. (c) Guijarro, A.; Yus, M. *The Origin of Chirality in the Molecules of Life: A Revision from Awareness to the Current Theories and Perspectives of This Unsolved Problem*; RSC Publishing: Cambridge, UK, 2009; pp 1−5.
(33) Hanson, K. R. *J. Am. Chem. Soc.* **1966**, *88*, 2731.
(34) Hirschmann, H.; Hanson, K. R. *J. Org. Chem.* **1971**, *36*, 3293.
(35) Hirschmann, H.; Hanson, K. R. *Tetrahedron* **1974**, *30*, 3649.
(36) Eliel, E. L. *Top. Curr. Chem.* **1982**, *105*, 1.
(37) Zabrodsky, H.; Avnir, D. *J. Am. Chem. Soc.* **1995**, *117*, 462.
(38) (a) Fujita, S. *J. Am. Chem. Soc.* **1990**, *112*, 3390. (b) Fujita, S. *J. Math. Chem.* **2012**, *50*, 2168. (c) Fujita, S. *Tetrahedron* **2006**, *62*, 691.
(39) Riant, O.; Hannedouche, J. *Org. Biomol. Chem.* **2007**, *5*, 873.
(40) Nozaki, K.; Sakai, N.; Nanno, T.; Higashijima, T.; Mano, S.; Horiuchi, T.; Takaya, H. *J. Am. Chem. Soc.* **1997**, *119*, 4413.
(41) Cahn, R. S.; Ingold, C.; Prelog, V. *Angew. Chem., Int. Ed. Engl.* **1966**, *5*, 385.
(42) Eliel, E. L.; Hargrave, K. D.; Pietrusiewicz, K. M.; Manoharan, M. *J. Am. Chem. Soc.* **1982**, *104*, 3635.
(43) Floss, H. G.; Tsai, M. D.; Woodard, R. W. In *Topics in Stereochemistry*; Allinger, N. L.; Eliel, E. L., Ed.; John Wiley & Sons: Hoboken, NJ, 1984; p 253.
(44) Nishiyama, H.; Kondo, M.; Nakamura, T.; Itoh, K. *Organometallics* **1991**, *10*, 500.
(45) Mestroni, G.; Alessio, E.; Zassinovich, G.; Marzilli, L. G. *Comments Inorg. Chem.* **1991**, *12*, 67.
(46) Sandoval, C. A.; Ohkuma, T.; Muniz, K.; Noyori, R. *J. Am. Chem. Soc.* **2003**, *125*, 13490.
(47) Trost, B. M.; Shen, H. C.; Dong, L.; Surivet, J. P. *J. Am. Chem. Soc.* **2003**, *125*, 9276.
(48) Pordea, A.; Creus, M.; Panek, J.; Duboc, C.; Mathis, D.; Novic, M.; Ward, T. R. *J. Am. Chem. Soc.* **2008**, *130*, 8085.
(49) Sheldrick, G. M. *SHELXS-97, Program for Crystal Structure Solution*; University of Göttingen: Germany, 1997.
(50) Sheldrick, G. M. *SHELXL-97, Program for Crystal Structure Refinement*; University of Göttingen: Germany, 1997.
(51) Gottarelli, G.; Lena, S.; Masiero, S.; Pieraccini, S.; Spada, G. P. *Chirality* **2008**, *20*, 471.
(52) Zhang, G. L.; Li, Y. T.; Luo, X. Q.; Wu, Z. Y. *Z. Anorg. Allg. Chem.* **2008**, *634*, 1161.
(53) Herwig, C.; Limberg, C. *Inorg. Chem.* **2008**, *47*, 2937.